

## Chemical Composition of Fumarolic Gases at the Menengai Geothermal Field- Central Rift Kenya: Variations monitored over a period of sampling from the year 2009 to June 2013

Leakey O. Auko, Jeremiah K. Kipngok, Geoffrey K. Mibei and Isaac K. Kanda

Geothermal Development Company, P.O Box 17700-20100, Nakuru-Kenya

lochieng@gdc.co.ke, jkipngok@gdc.co.ke gmibei@gdc.co.ke and ikanda@gdc.co.ke

**Keywords:** Fumaroles, atmospheric contamination, geothermometer, variation.

### ABSTRACT

Physico-chemical characteristics of the fluids circulating in a volcanic system can display significant temporal variations, in response to changes caused by different inputs of: condensation attributed to atmospheric contamination, boiling, as well as re-equilibration in response to cooling and reactions between juvenile (magmatic) and more surficial (hydrothermal and meteoric) components during the fluid ascend to the surface. This paper seeks to outline the temporal variation of the gas concentrations ( $\text{CO}_2$ ,  $\text{H}_2\text{S}$ ,  $\text{H}_2$ ,  $\text{CH}_4$ ,  $\text{O}_2$  and  $\text{N}_2$ ) detected in Fumaroles MF-2, MF-3, MF-7 and MF-9 during a period of sampling from 2009 to June, 2013. The sampling temperatures of the different fumaroles range from 56°C to 90 °C depending on the fumarole discharge strength. The Menengai fumarolic gas flow is propelled to the surface along well-formed conduits of faults and fissures that characterize the superposed lava. This invariably gives rise to the atmospheric contamination of the gases over the different phases of sampling, ultimately affecting the chemistry of the gas species through condensation and/or boiling at the time of sampling. The varying relative concentration of  $\text{CO}_2$ ,  $\text{H}_2\text{S}$  and  $\text{N}_2$  in the subsequent sampling phases could be primarily due to condensation caused by atmospheric contamination. The predominant surficial atmospheric contamination makes it difficult to constrain the temporal variation in response to any physicochemical processes happening in the reservoir that can be discernible in the surface thermal expressions. The average computed equilibrium reservoir temperatures are of the order of magnitude of 270°C and above 300°C with respect to  $\text{H}_2\text{S}$  and  $\text{CO}_2$  geothermometers respectively. The temperatures calculated from the same functions in the subsequent phases of sampling give markedly lower temperatures with an exception of  $\text{CO}_2$  geothermometer which was >350°C.

### 1. INTRODUCTION

Many fundamental concerns arise regarding any possible effect of geothermal development in Menengai geothermal field on the fumarolic discharges in the caldera. This paper seeks to evaluate the temporal changes in the fumarole discharge chemistry. In respect to this subject, many researchers (e.g.; Tedesco and Sabroux, 1987; Martini, 1989; Giggenbach, 1996; Tassi et al., 2003; Shinohara, 2013) have emphasized the importance of monitoring the chemical composition of volcanic gases and waters to forecast changes in volcanic activity. This is as a good geohazard monitoring practice. It is also well known (e.g. Tassi et al., 2003; Gerlach and Nordlie, 1975) that the physicochemical characteristics of the fluids circulating in a volcanic system can display significant temporal variations, in response to changes induced by inputs of deep and shallow processes. The fumaroles studied in this paper are MF-2, MF-3, MF-7 and MF-9 (Figure 1) based on the availability of data over the specific period of study. The selected fumaroles are located closely to some drilled wells in Menengai, for instance MF-2 is near MW-15, MF-3 is near MW-20, MF-7 is near MW-04 and MF-9 is near MW-10 (Figure 1).

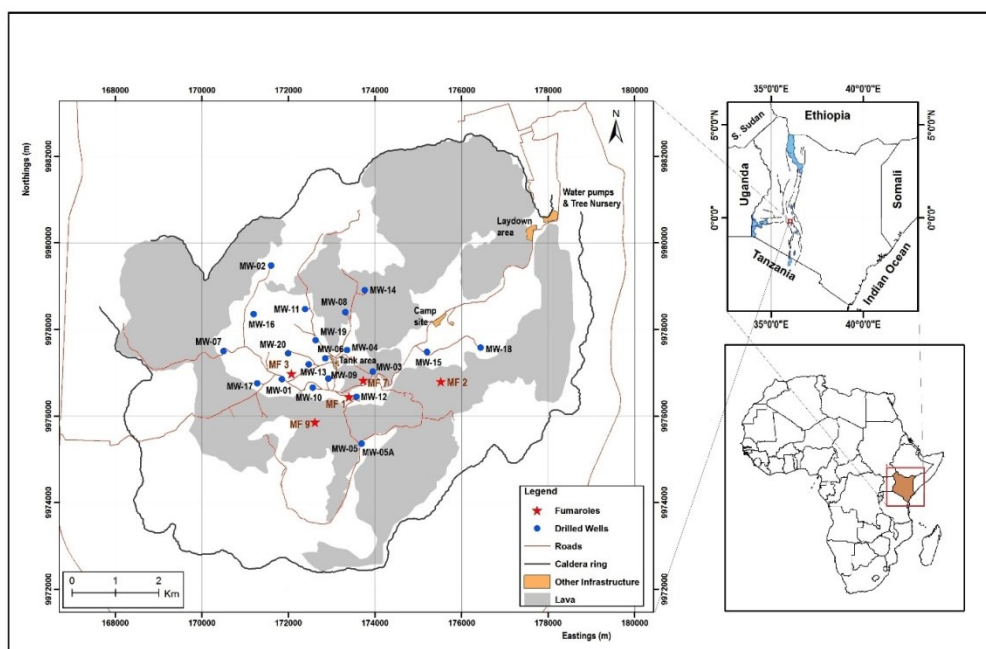


Figure 1: Location of the Menengai Fumaroles

## 2. GEOLOGICAL SETTING

Menengai caldera is characterized by partly superposed trachytic lava flows of different ages, covering virtually the entire caldera floor. Several studies (e.g. McCall, 1967; MacDonald et al., 1970; Griffith, 1977; Jones & Lippard, 1979; Jones, 1985; Griffith, 1980; Griffith and Gibson, 1980; Leat, 1983, 1984, 1985; Williams et al., 1984; Geotermica Italiana Srl, 1987; MacDonald et al., 1994; Mungania et al., 2004; Lagat et al., 2010) on the surface geology of Menengai have been carried out for various reasons. All these studies have underpinned that Menengai is a late Quaternary volcano, which has produced trachyte and pantellerites volcanics. They comprise pyroclastics and lava flows with most of the surface adjacent to Menengai caldera being covered by extensive pyroclastics, which accompanied the caldera collapse. The surface is covered by volcanic rocks mostly erupted from centres within the area. Most of the area around the caldera is covered by mainly pyroclastics erupted from centres associated with Menengai volcano. Young lava flows infilling the main caldera are post caldera in age. Older (Pleistocene) lavas mainly trachytic and phonolitic in composition and are exposed in the northern parts and are overlain by eruptives from Menengai volcano. Some alluvial deposits are found in low-lying narrow grabens where they are deposited as thin reworked layers. One isolated exposure of diatomaceous bed is noted on the caldera floor, probably indicative of prehistoric climates and existence of shallow fresh water lakes in this part of the rift.

## 3. SAMPLING AND ANALYSIS

The sampling procedures are those described by Arnórsson et al. (2006). The fumarole discharge was trapped using a plastic funnel whose contact points with the ground were sealed with mud to prevent any contamination with atmospheric air. The fumarole gases were sampled by directing the steam into a pre-weighed evacuated Giggenbach gas flask containing 50 ml of 40% w/v NaOH solution, with cold water continuously poured on top of the flask to cool it. The acidic gases ( $\text{CO}_2$  and  $\text{H}_2\text{S}$ ) were absorbed into the NaOH solution giving room in the evacuated flask for the other non-condensable gases ( $\text{CH}_4$ ,  $\text{H}_2$ ,  $\text{N}_2$  and  $\text{O}_2$ ) usually found in thermal fluids to concentrate to measurable levels. The acidic gases,  $\text{CO}_2$  and  $\text{H}_2\text{S}$ , were analyzed titrimetrically using 0.1M HCl and 0.001M mercuric acetate while the other non-condensable gases ( $\text{CH}_4$ ,  $\text{H}_2$ ,  $\text{N}_2$  and  $\text{O}_2$ ) were analyzed by gas chromatograph. Generally, sample collection and analysis was done as described by Ármannsson and Ólafsson, 2006.

## 4. RESULTS AND DISCUSSIONS

### 4.1 Fumarole Gas Chemistry

Menengai Caldera is essentially characterized by numerous steaming grounds and fumaroles, which signify the presence of geothermal activity. The entire caldera floor is covered by predominantly trachytic lava, which is punctuated by fissures and fractures depending on the varying ages of lava superposition. This leaves no doubt on the possible effect of atmospheric air contamination to the general Menengai fumarolic gas chemistry which is indeed demonstrated by the high  $\text{N}_2$  and  $\text{O}_2$  concentrations in the gas species rendering  $\text{H}_2$  and  $\text{CH}_4$  being zero. Hence this, observation is reminiscent in all the samples collected and analysed from the year 2009 to 2013. This paper outlines the temporal variation of the gas concentrations ( $\text{CO}_2$ ,  $\text{H}_2\text{S}$ ,  $\text{H}_2$ ,  $\text{CH}_4$ ,  $\text{O}_2$  and  $\text{N}_2$ ) detected in Fumaroles MF-2, MF-3, MF-7 and MF-9 for a period of sampling from the year 2009 to March, 2013 (Table 1).

**Table 1: Fumarole gas chemistry results**

Fumarole Number	Coordinates		Samp	pH/T°C	$\text{CO}_2$	$\text{H}_2\text{S}$	$\text{H}_2$	$\text{CH}_4$	$\text{N}_2$	$\text{O}_2$
	Northings	Eastings	temp		mmol/kg					
<b>December, 2009</b>										
MF2	9976778	175516	88	8	1176.8	5	0	0	12014	3209
MF3	9975855	172610	85	7.7	5869	7.22	0	0	15037.2	4019
MF7	9976673	173745	88	7	6246	23.3	0	0	35112.4	9469
MF9	9976425	172582	70	7.8	6766	13.9	0	0	33912.9	8729
<b>September, 2012</b>										
MF2	9976778	175516	90.9	6.4/23.3	471	0.011	0	0	2004	466
MF3	9975855	172610	78.6	8.9/21.6	1580	0	0	0	1603	373
MF7	9976673	173745	79.3	7.9/20.9	459	0.019	0	0	1486	350
MF9	9976425	172582	69.5	6.5/24.5	346	0.043	0	0	1699	399
<b>March, 2013</b>										
MF2	9976778	175516	90.3	6.7/24.3	623	0.014	0	0	703	161
MF3	9975855	172610	78.9	8.6/24.4	933	0.027	0	0	1354	313
MF7	9976673	173745	79.4	7.0/23.5	6728	5.079	0	0	16165	3736
MF9	9976425	172582	68.7	6.4/24.6	7366	1.706	0	0	32379	7463

The outlet temperatures of the different Menengai fumaroles range from 56°C to 90°C which is attributed to a varying degree of atmospheric contamination. The selected fumaroles have an outlet temperature in the range of about 68°C to 90°C. The sampling temperatures of the fumaroles over the three phases of sampling generally show a slight decreasing trend. However, the variation could be negligible, within the acceptable error margin, or could be attributed to the varying stability of the measuring thermocouple at the time of sampling.

#### 4.2 Evaluation of temporal changes in Menengai Fumarolic Gas Composition

Changes in the chemical composition of Menengai fumarolic gas species accessible to sampling from the year 2009 to 2013 can conveniently be investigated using the ternary plots of  $\text{H}_2\text{O}-\text{CO}_2-\text{N}_2$  (Figure 2) and  $\text{H}_2\text{O}-\text{CO}_2-\text{H}_2\text{S}$  (Figure 3) as discussed by Marini (2004). The two ternary diagrams have been plotted on the principle of the two major chemical components,  $\text{H}_2\text{O}$  and  $\text{CO}_2$ , plotted together with another gas species, such as  $\text{N}_2$  and  $\text{H}_2\text{S}$ . This makes it conveniently easy to infer the effects of interfering processes (e.g., addition of atmospheric air, oxidation of reduced gas species, and steam condensation) which are invariably taken into account (Marini, 2004; Marini, 2014).

##### 4.2.1 Triangular plot of $\text{H}_2\text{O}-\text{CO}_2-\text{N}_2$ for Menengai Fumarolic gases

The  $\text{H}_2\text{O}-\text{CO}_2-\text{N}_2$  triangular of the selected Menengai fumaroles complimented by fumarolic gas data (Table 1) provides a great insight into deducing the rampant incursion of atmospheric air to fumarolic fluids in Menengai. This could be due to either inflow of atmospheric gases that are propelled by fissures, faults and fractures cutting the superposed lava to the fumarolic conduits streaming up to the sampling point and or even coupled by slight air contamination during sample collection. The samples collected at different phases cluster into two categories:

- i. The samples that are slightly affected by atmospheric incursion and tend to plot away from  $\text{N}_2$  apex but towards  $\text{H}_2\text{O}$  apex. This is particularly visible in the fumarole samples collected in September 2012 (rectangle symbols) and MF-2 and MF-3 collected in March 2013 (diamond symbols).
- ii. The samples that are adversely affected by atmospheric incursion and tend to plot towards the  $\text{N}_2$  apex but away from  $\text{H}_2\text{O}$  apex. This is manifested by virtually all the samples collected in the year December, 2009 with MF-2 being near the transition line. In addition, the fumaroles MF-7 and MF-9 collected in March 2013 also show significantly high atmospheric contamination and have considerably high  $\text{CO}_2$  content.

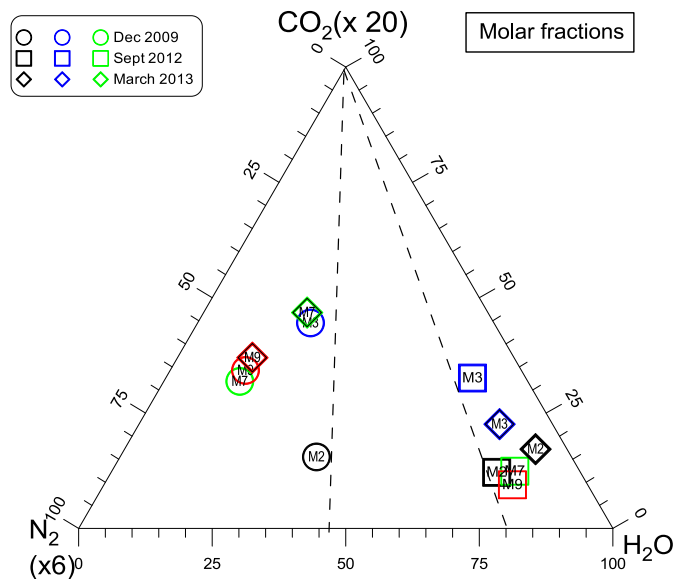


**Figure 2: Triangular plot of  $\text{H}_2\text{O}-\text{CO}_2-\text{N}_2$  for Menengai fumaroles MF-2 (black symbols), MF-3 (blue symbols), MF-7 (green symbols) and MF-9 (red symbols) sampled between the years 2009-2013**

##### 4.2.2 Triangular plot of $\text{H}_2\text{O}-\text{CO}_2-\text{H}_2\text{S}$ for Menengai Fumarolic gases

Apparently the selected Menengai fumaroles collected in December, 2009 and MF-7 and MF-9 collected in March, 2013 which show high entrainment of atmospheric gas cluster towards the  $\text{H}_2\text{S}$  apex in the  $\text{H}_2\text{O}-\text{CO}_2-\text{H}_2\text{S}$  triangular plot (Figure 3). Samples with appreciable amounts of  $\text{H}_2\text{S}$  (1-23 mmole/kg) that cluster around the  $\text{H}_2\text{S}$  apex were obtained from all the fumaroles in December 2009 and MF-7 and MF-9 in March 2013. In principle this is rather unanticipated since addition of atmospheric gases should cause a decrease in  $\text{H}_2\text{S}$  concentration due to its  $\text{O}_2$ -driven oxidation to elemental sulfur or other oxidized species coupled by condensation. Marini (2014) observed similar pattern for the Dunkley et al. (1993) Silali fumarole samples 220 and 223. These Menengai samples tend to have low  $\text{CO}_2/\text{H}_2\text{S}$  ratio ranging from 230-4300. MF-2 that lies more or less in the transition zone has a  $\text{CO}_2/\text{H}_2\text{S}$  ratio of about 236 attributed to its least  $\text{CO}_2$  content. The low  $\text{CO}_2/\text{H}_2\text{S}$  ratio in these set of samples is primarily due to the entrainment of atmospheric gases and low degree of condensation.

Samples with near zero or zero amounts of  $\text{H}_2\text{S}$  cluster along the  $\text{H}_2\text{O}-\text{CO}_2$  line and are generally shown in all the fumaroles samples collected in September 2012 (rectangle symbols) and MF-2 and MF-3 collected in March 2013 (diamond symbols). These samples suffered mild atmospheric contamination but have considerably low  $\text{H}_2\text{S}$  content which is equally unexpected. They are marked by significantly high  $\text{CO}_2/\text{H}_2\text{S}$  ratio due to the low value of  $\text{H}_2\text{S}$  denominator. It is well known (e.g. Nicholson, 1993) that gases such as  $\text{NH}_3$ ,  $\text{H}_2$  and  $\text{H}_2\text{S}$  are removed from the steam by wall-rock reactions and solution into steam condensate (particularly for the more soluble gases e.g.  $\text{NH}_3$  and  $\text{H}_2\text{S}$ ). This coupled with the atmospheric incursion that consequently oxidizes  $\text{H}_2\text{S}$  can primarily account for the low absolute  $\text{H}_2\text{S}$  content which ultimately leads to the elevated  $\text{CO}_2/\text{H}_2\text{S}$  ratio. These fumaroles might have suffered high degree of condensation.

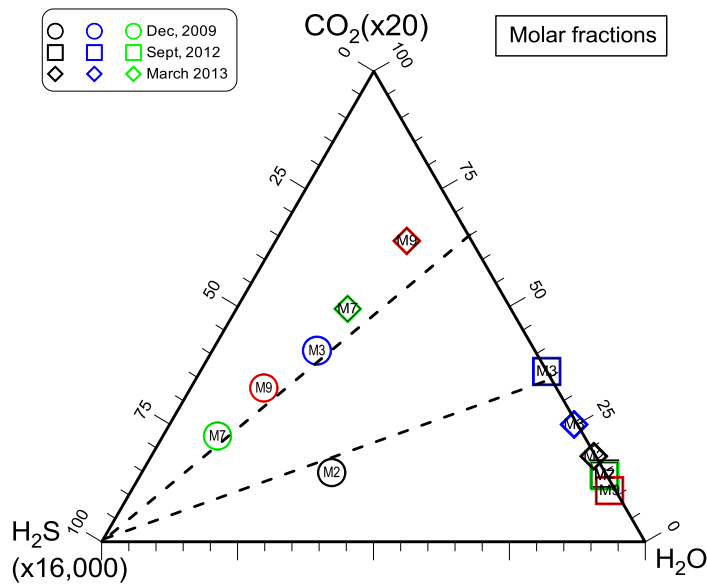


**Figure 3: Triangular plot of  $\text{H}_2\text{O}-\text{CO}_2-\text{H}_2\text{S}$  for Menengai fumaroles MF-2 (black symbols), MF-3 (blue symbols), MF-7 (green symbols) and MF-9 (red symbols) sampled between the years 2009-2013**

#### 4.3 Preliminary evaluation of fumarolic steam condensation

There is unclear pattern observed in the variation in the concentrations of the fumarolic gas species (e.g.  $\text{CO}_2$ ,  $\text{H}_2\text{S}$ ,  $\text{N}_2$  and  $\text{O}_2$ ) that could exist because of varying degree of atmospheric contamination at depth coupled by sampling procedures leading to entrainment of air during the three phases of sampling. Varying degree of fumarolic steam condensation close to the surface might have played a significant role in the absolute gas composition over the different periods of sampling. Nicholson (1993) affirmed that condensation removes water vapor from the steam flow resulting in higher total-gas proportion in the vapor phase (i.e. higher gas/steam ratio), which increases with increasing condensation. Two processes; conductive heat loss and mixing with cold water were considered to primarily account for the steam condensation as thermal fluids ascent to the surface while putting into account various thermodynamic assumptions (Arnórsson, 1987). The relative concentration of  $\text{CO}_2$  and  $\text{N}_2$  can conveniently be used to investigate the condensation processes. In principle  $\text{CO}_2$  is more soluble in water than  $\text{N}_2$ , hence primary boiling involving partial degassing will cause the remaining water to attain a high  $\text{CO}_2/\text{N}_2$  ratio for its temperature as well as the steam formed by extensive boiling of this water. Re-equilibration of partly degassed water with respect to  $\text{CO}_2$  would also augment the  $\text{CO}_2/\text{N}_2$  (Arnórsson, 1987). There is an irregular pattern in the relative  $\text{CO}_2$  and  $\text{N}_2$  content as well as the  $\text{CO}_2/\text{N}_2$  ratio from the three sampling phases of the Menengai fumaroles primarily due to the varying magnitude of contamination and condensation. Nevertheless, it can be postulated that the primary boiling involving partial degassing compounded by extensive boiling could account for the  $\text{CO}_2/\text{N}_2$  ratio which is in the region of 0.4 to 4 units.

#### 4.4 Relative composition of gas species

##### 4.4.1 $\text{CO}_2$ concentration in the Menengai Fumaroles

In December 2009,  $\text{CO}_2$  concentration in the fumaroles was on the order of 14% of the total gas content, which ranges from 1176 to 6766 mmole/kg. Subsequent sampling in September, 2012 showed a varying decline in  $\text{CO}_2$  concentration in the fumaroles with MF-9 having the lowest concentration of about 346mmole/kg which ultimately depended on the various degree of atmospheric contamination at the subsurface which consequently led to steam condensation. Nonetheless, the low concentration of  $\text{CO}_2$  (Figure 4) constituted 24% of the total gas. In March 2013,  $\text{CO}_2$  concentration in the fumaroles was about 30% of the total gas, which ranged from 623 to 7366 mmole/kg, with MF-9 having the highest  $\text{CO}_2$  concentrations of about 7366 mmole/kg.

The source of the  $\text{CO}_2$  in Menengai fumaroles is likely to be of magmatic origin, however this deduction need to be affirmed by isotopic studies. Other sources of  $\text{CO}_2$  gas can be produced by thermal alteration of carbonate rocks and minerals from the degradation of organic matter within sedimentary rocks at depth or in near-surface reactions, and from solutes in meteoric waters (notably the conversion of  $\text{HCO}_3$  (aq) to  $\text{CO}_2$  (g) on boiling) (Nicholson, 1993).

By comparing the fumarole  $\text{CO}_2$  composition sampled from 2009 to 2013, it is obvious that the  $\text{CO}_2$  content (Figure 4) show a considerable increase in 2013. However, MF-9 sampled in 2012 show a slight variation that probably relates to sampling and atmospheric contamination as earlier observed. It is commonly known that oxygen signature in geothermal gases clearly depicts addition of atmospheric air into the thermal gases, therefore this is the basis of comparing the relative  $\text{CO}_2$  and  $\text{O}_2$  content.

##### 4.4.2 $\text{H}_2\text{S}$ concentrations in the Menengai Fumarolic gases

Generally,  $\text{H}_2\text{S}$  content in the fumaroles is markedly low, and the concentration ranges from 0 to 23 mmole/kg of the total gas composition over the periods of sampling. The  $\text{H}_2\text{S}$  composition was 0.03%, 0.001% and 0.006% in 2009, 2012 and 2013 respectively. High solubility of  $\text{H}_2\text{S}$  in the liquid phase (shallow ground water and or fumarole steam) and the imminent oxidation during the ascent to the surface may account for the low  $\text{H}_2\text{S}$  content in the Menengai fumaroles. In principle, the solubility of a gas in the liquid phase of a geothermal fluid governs the extent to which it fractionates into the vapour phase on steam formation.  $\text{H}_2\text{S}$

is 2-3 times more soluble than carbon dioxide (Nicholson, 1993). Steam condensation near the surface of the fumarole upstream conduit primarily caused by entrainment of atmospheric air has a considerable effect to the highly soluble H<sub>2</sub>S content.

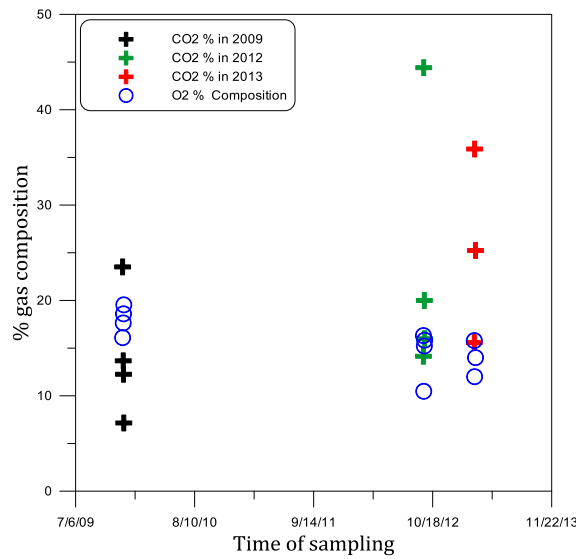


**Figure 4: % CO<sub>2</sub> gas composition in relation to total gas content**

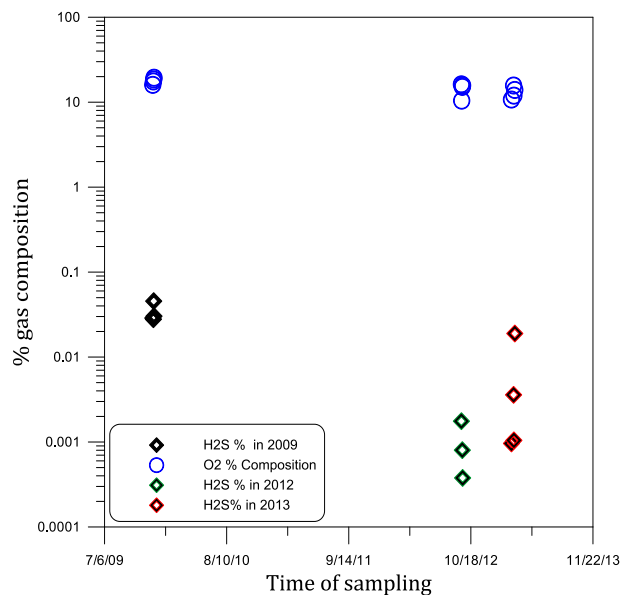


**Figure 5: % H<sub>2</sub>S gas composition**

At a given O<sub>2</sub> fugacity, sulfur occurs as SO<sub>2</sub> at high temperature and as H<sub>2</sub>S at lower temperature (Lee et al., 2008). Giggenbach (1987) suggested that Eq. (1) is important for a degassing magma during its ascend towards the surface.



Thermodynamic modeling indicates that the reaction shifts to the right at high pressures (i.e. the magma degasses at great depths), thus H<sub>2</sub>S is the dominant sulfur species in the gas. Conversely, hot gases escaping from a magma body emplaced at shallow levels in the crust will tend to be SO<sub>2</sub>-dominated (Giggenbach, 1987). H<sub>2</sub>S is primarily present in Menengai fumaroles, and the origin is likely to be magmatic. In addition, Nicholson (1993) underscored that H<sub>2</sub>S may be produced by alteration of the reservoir rocks or from a magmatic source. It is reactive and is removed on reaction with wall rocks to form iron sulphides. Although this appears to be a slow process, the gas is lost through such reactions over time, increasing the CO<sub>2</sub>/H<sub>2</sub>S ratio with increased migration.

#### 4.4.3 Comparative concentration of CO<sub>2</sub> and H<sub>2</sub>S

The relative concentration of CO<sub>2</sub> and H<sub>2</sub>S is principally controlled by the water solubility factors which determine the component fractionation into the steam phase. It is evident that the fumarolic discharge is enriched in more CO<sub>2</sub> than H<sub>2</sub>S, which is attributed to the high solubility of H<sub>2</sub>S upon boiling during its ascent to the surface and compounded by condensation as the fluids ascent to the

surface, as well as atmospheric contamination. This prevalent contamination makes it difficult to recognize the temporal variation in response to any physicochemical processes happening in the reservoir.

The  $\text{CO}_2/\text{H}_2\text{S}$  ratio has been suggested to be a useful proxy for identifying upflow zones, subsurface flow of boiling water, and identify their sources (Arnórsson, 1987, Nicholson, 1993 Gigganbach, 1992, 1996). In 2009, the  $\text{CO}_2/\text{H}_2\text{S}$  ratio of the fumaroles was considerably low value while the  $\text{H}_2\text{S}/\text{CO}_2$  was high due to the somewhat high  $\text{H}_2\text{S}$  concentrations caused by condensation factors. In the subsequent years of sampling: 2012 and 2013, the  $\text{CO}_2/\text{H}_2\text{S}$  ratio was markedly high while on the other hand the  $\text{H}_2\text{S}/\text{CO}_2$  ratio was considerably low due to the low  $\text{H}_2\text{S}$  contents occasioned by mild degree of atmospheric contamination.

#### 4.4.4 Comparative $\text{H}_2$ and $\text{CH}_4$ concentration in the Menengai Fumaroles

$\text{H}_2$  is indeed a highly reactive gas, and is readily removed during reaction with rocks. It is commonly lost over time and with increased migration (Arnórsson and Gunnlaugsson, 1985). The Menengai fumaroles gas composition generally shows an absence of  $\text{H}_2$  during the period of sampling. The atmospheric contamination and ultimate high  $\text{H}_2$  reactivity is the reason that suffices the explanation for this observation.

$\text{CH}_4$ -rich gases can be formed under the low temperature hydrothermal conditions surrounding the high-temperature magmatic system (Gigganbach, 1987). The  $\text{CH}_4$  solubility in liquid water at temperatures  $< 100^\circ\text{C}$  decreases in the order  $\text{CH}_4 > \text{H}_2 > \text{CO}$ . During Rayleigh-type condensation,  $\text{CH}_4$  is invariably removed most effectively from the residual vapor phase (Marini and Fiebig, 2004) and this could also account for the zero content of  $\text{CH}_4$  in the Menengai fumarolic gas. Menengai fumarolic gases are generally poor in  $\text{CH}_4$  this is primarily due to the prevalent atmospheric contamination and condensation factors.

#### 4.4.5 $\text{N}_2$ and $\text{O}_2$ concentrations in the Menengai Fumarolic gases

$\text{N}_2$  and  $\text{O}_2$  are the principal atmospheric gases. Most nitrogen in geothermal systems is derived from that dissolved in the meteoric recharge waters, although it can also be of magmatic origin. The presence of oxygen in a gas sample often indicates contamination either by soil air or during the sampling procedure (Nicholson, 1993). Menengai is characterized by partly superposed lava flows of different ages, covering virtually the entire caldera floor. The Menengai fumarolic field is characterised by fractures and fissures and some areas punctuated by highly hydrothermally altered rocks. This promotes air circulation and air mixing with the ascending volcanic gases. It is with regard that  $\text{N}_2$  and  $\text{O}_2$  constitutes the highest percentage of the total gas in the fumaroles; in 2009, the average  $\text{N}_2$  and  $\text{O}_2$  content was 68% and 18% respectively of the total gas composition. The average  $\text{N}_2$  and  $\text{O}_2$  content in 2012 and 2013 is 62%, 14% and 57%, 13% respectively. Therefore, there is generally a decreasing trend in the  $\text{N}_2$  and  $\text{O}_2$  content over the three phases of sampling which implies a decreasing magnitude of atmospheric air circulation and contamination during sampling. The sampling techniques, varying concentration of other gases ( $\text{CO}_2$  and  $\text{H}_2\text{S}$ ), and varying degree of atmospheric contamination coupled with varying degree of steam condensation could be the reason for the varying  $\text{N}_2$  and  $\text{O}_2$  content. It could also be worthwhile to complement this observation with  $\text{N}_2/\text{Ar}$  ratio so as to get more insight of atmospheric air contamination.

### **4.5. Model of the formation, composition and variation of the Menengai Fumarolic gas species**

The typical model of formation of Menengai fumaroles could be the ubiquitous model of the formation thermal fluids in a volcanic system as suggested by Nicholson (1993). Multiple studies (e.g. Mizutani and Matsuo 1959; Gerlach and Nordlie, 1975; Gigganbach, 1996; Churakov et al., 2000; Saito et al., 2002; Tassi et al., 2003; Marini, 2004; Lee et al., 2008) have established that the physicochemical characteristics of fluids in volcanic systems can significantly vary in response to deep and shallow processes. Therefore, the main deep process is primarily the vapour melt separation during the generation and rise of the magmas. The variations in composition of the gases are due to shallow/secondary processes such as condensation and/or boiling at the time of sampling, mixing with shallow aquifer, re-equilibration in response to cooling and dilution by meteoric water, and interaction with fluids associated with hydrothermal systems (secondary hydrothermal system (SHS)). The volcanic gas composition can provide an important indicator of magmatic plumbing and degassing conditions that help to monitor volcanic activities (Shinohara, 2013). In addition different studies (e.g. Gigganbach, 1997; Churakov et al., 2000) have deduced that volcanic gas composition and the components of the gas phase are normally in thermodynamic equilibrium at the temperature of sampling. If the thermodynamic equilibrium is constrained, it can help in developing a correct model of evolution of the gas composition.

In the context of Menengai, it can be postulated that the Menengai fumarolic gases are formed as a result of degassing magma during vapour melt separation coupled by boiling in the two-phase zone of the geothermal reservoir. The degassing magma body that is predominantly of a trachytic melt produced through fractional crystallization from a parent basaltic magma. The fumaroles show a low flow rate and outlet temperature actually does not show any significant variation during the three phases of sampling, (the slight temperature variation is within the analytical error). The fumarolic discharge contains  $\text{H}_2\text{O}$  with a  $\delta\text{D}$  value close to 10‰ to -20‰ for fumarole discharge (Geotermica Italiana Srl, 1987) which correlates with  $\delta\text{D}$  value of -15.7 ‰ for well MW-04 condensate (Sekento, 2012). The gas composition is modified by the shallow aquifer, varying degree of atmospheric contamination and steam condensation and the gas flow is greatly propelled to the surface along well-formed conduits of faults and fissures that characterize the partly layered lava. A minor variation is recorded in gas species ( $\text{CO}_2$ ,  $\text{H}_2\text{S}$ ,  $\text{N}_2$  and  $\text{O}_2$ ) over the different phases of sampling. In addition, there is no observable crop up of new or increased fumarolic activity.

### **4.6. Equilibrium reservoir temperature**

The estimated gas equilibrium reservoir temperatures applied to the Menengai fumarolic gases are functions of Arnórsson and Gunnlaugsson (1985) for  $\text{TCO}_2$ , and  $\text{TH}_2\text{S}$ , while  $\text{TCO}_2$  and  $\text{TH}_2\text{S}$  are from Arnórsson et al. (1998) and  $\text{TH}_2\text{S}-\text{CO}_2$  from Nehring and D'Amore (1984) respectively (Figure 6). The average gas geothermometer temperatures calculated from the samples collected in 2009 are in the order of above  $350^\circ\text{C}$ , above  $270^\circ\text{C}$ , and above  $290^\circ\text{C}$  for  $\text{TCO}_2$ ,  $\text{TH}_2\text{S}$  and  $\text{TH}_2\text{S}-\text{CO}_2$  respectively. These findings were similarly underscored by (e.g. Lagat et al., 2010; Kanda, 2011) where the author found that the  $\text{TH}_2\text{S}$  geothermometer gave temperatures ranging from  $279^\circ\text{C}$ - $296^\circ\text{C}$  while  $\text{TH}_2\text{S}-\text{CO}_2$  gave temperatures ranging from  $274^\circ\text{C}$  - $304^\circ\text{C}$ . The temperatures calculated from the same functions in the subsequent phases of sampling gave a markedly lower temperatures with an exception of  $\text{TCO}_2$  which was  $>350^\circ\text{C}$ . The differences in equilibrium temperatures calculated with the  $\text{TCO}_2$ ,  $\text{TH}_2\text{S}$  and  $\text{TH}_2\text{S}-\text{CO}_2$  geothermometers suggest that thermodynamic gas equilibria are not reached at the temperature of sampling (e.g.

Giggenbach, 1991, 1993). In addition, the unrealistically low values of the calculated  $\text{H}_2\text{S}$  temperature during the second phase of sampling in 2012 could be as a result of the atmospheric component that affects the circulation system, as also shown by the presence of  $\text{N}_2$  and  $\text{O}_2$  content.

The atmospheric contamination of the Menengai fumarolic gas discharge has so far rendered the values of  $\text{CH}_4$  and  $\text{H}_2$  to be zero thus making it hard to investigate the Fayalite-Hematite-Quartz (FHQ) redox buffer conditions given by Giggenbach (1987) with respect to the diagram of  $\log(\text{CH}_4/\text{CO}_2)$  vs.  $\log(\text{H}_2/\text{H}_2\text{O})$ .

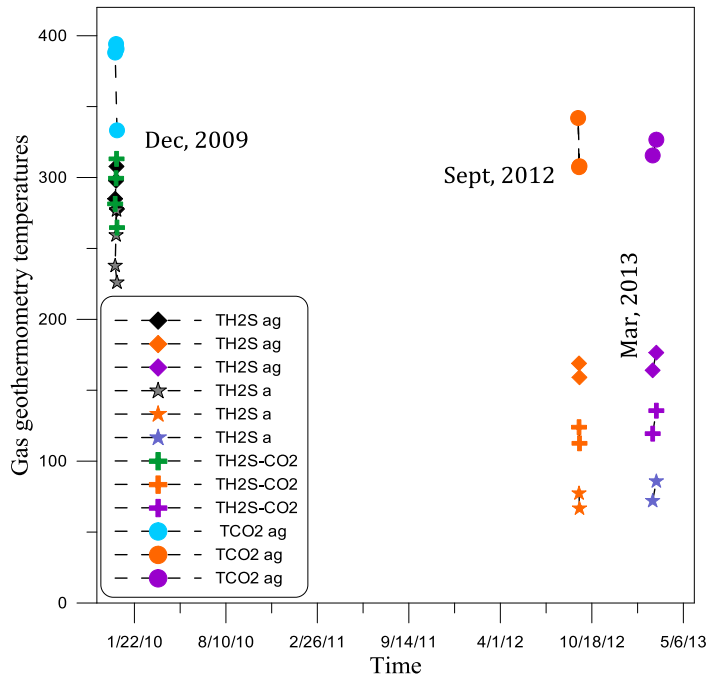


**Figure 6: Equilibrium reservoir temperature, where ag: Arnorsson & Gunnlaugsson (1985), a: Arnorsson et al. (1998) and TH2S-CO2: Nehring and D'Amore (1984)**

## 5. CONCLUSIONS

- The outlet temperatures of the Menengai fumaroles range from 56°C to 90°C and are marked by significantly low flow rates.  $\text{N}_2$  and  $\text{O}_2$  constitutes on average over 75% of the total gas composition indicating high atmospheric input. On average,  $\text{CO}_2$  comprises about 25% while  $\text{H}_2\text{S}$  is virtually near zero.
- The varying degree of atmospheric contamination and condensation is notably vital in determining the overall composition of the fluids.  $\text{H}_2\text{O}$  constitutes about 60-95% of the total proportion of fumarolic discharge fluids,  $\text{N}_2+\text{O}_2$  on average constitutes 2- 40%,  $\text{CO}_2$  comprises about 1-7% while  $\text{H}_2\text{S}$  accounts for near zero of the total fluids due to its high solubility in water
- The predominant atmospheric contamination makes it practically difficult to record the temporal variation in composition of fumaroles' discharge in response to any physicochemical processes happening in the reservoir
- Nonetheless, there is neither a significant observable increase in concentration of species dissolved in the fluids over time nor any decrease in new thermal manifestations in response to the development of the field.
- The estimated gas equilibrium reservoir temperature is the range of 270 to >350°C based on the Menengai fumarolic gas chemistry. The strikingly high calculated  $\text{TCO}_2$  temperature > 350°C can be due to the relatively high  $\text{CO}_2$  content that is invariably subdued by the atmospheric incursion

## REFERENCES

Ármannsson, H. and Ólafsson, M.; Collection of geothermal fluids for chemical analysis. ISOR 2006 report (2006).

Arnórsson S.: Gas chemistry of the Krisuvík geothermal field iceland with special reference to evaluation of steam condensation in the upflow zones , *Jökull*, vol. 37, (1987) 31-47,

Arnórsson S. and Gunnlaugsson E., 1985: New gas geothermometers for geothermal exploration-calibration and application, *Geochem. Cosmochim. Acta* 49, 1307-1375.

Arnórsson, S., Andrésdóttir, A., Gunnarsson, I., and Stefánsson, A.: New calibration for the quartz and Na/K geothermometers – valid in the range 0-350°C, *Proceedings, Geoscience Society of Iceland Annual Meeting*, (1998), 42-43.

Arnórsson, S.; Chemistry of gases associated with geothermal activity in Iceland: A Review. *Journal of Geophysical Research*, Vol. 91, (1986), 12261-12268.

Arnórsson, S., Bjarnason, J.Ö., Giroud, N., Gunnarsson, I., and Stefánsson, A., 2006: Sampling and analysis of geothermal fluids. *Geofluids*, **6**, 203-216

Churakov, S. V., Tkachenko S. I., Korzhinskii, M. A., Bocharnikov, R. E. and Shmulovich, K. I.: Evolution of Composition of High-Temperature Fumarolic Gases from Kudryavy Volcano, Iturup, Kuril Islands: the Thermodynamic Modeling, *Geochemistry International*, **Vol. 38**, No. 5, 2 pp. (2000), 436-451

Dunkley P.N, Smith M, Allen D J, Darling, W, G.; Geothermal activity and geology of the northern sector of the Kenya Rift Valley, Kenya Ministry of Energy, *British Geological Survey Research Report SC/93/1* (1993).

Geotermica Italiana Srl,: Geothermal reconnaissance survey in the Menengai- Bogoria area of the Kenya Rift Valley. *UN (DTCD)/ GOK* (1987)

Gerlach, T.M., Nordlie, B.E.,: The C-O-H-S gaseous system part I: composition limits and trends in basaltic cases. *Am. J. Sci.* **275**, (1975), 353-376.

Giggenbach, W.F.,: Redox processes governing the chemistry of fumarolic gas discharges from White Island, New Zealand. *Appl. Geochem.* **2**, (1987), 143-161

Giggenbach, W.F., Chemical techniques in geothermal exploration. In: Application of Geochemistry in Geothermal Research. *UNITAR*, (1991), pp 119-144.

Giggenbach, W.F., Isotopic and chemical compositions of water and steam discharges from volcanic-magmatic-hydrothermal systems of the Guanacaste Geothermal Province, Costa Rica. *Appl. Geochem.* **7** (1992), 309-332.

Giggenbach, W.F.: Redox control of gas composition in the Philippine volcanic-hydrothermal system. *Geothermics*, **22**, (1993) 575-587.

Giggenbach, W.F., Chemical composition of volcanic gases. In: Scarpa, M., Tilling, R. (Eds.), Monitoring and Mitigation of Volcanic Hazards. *Springer, Berlin*, (1996), pp. 221-256.

Giggenbach, W.F., "The origin and evolution of fluids in magmatic-hydrothermal systems," in *Geochemistry of Hydrothermal Ore Deposits*, 3rd edition, H.L. Barnes ed., John Wiley and Sons, NY, June (1997).

Griffith P. S.,: The geology of the area around Lake Hannington and the Perkerra River Rift Valley Province, Kenya. *PhD thesis, University of London*. (1977)

Griffith P. S.: Box fault systems and ramps: Atypical association of structures form the eastern shoulder of the Kenya rift. *Geol. Mag.*, (1980), 579-586 pp.

Griffith P. S., and Gibson I. L.: The geology and the petrology of the Hannington Trachyphonolite formation, Kenya Rift Valley. *Lithos*, **13**, (1980) 43-53 pp

Jones, W.B.,: Discussion on geological evolution of trachytic caldera and volcanology of Menengai volcano, Rift Valley, Kenya. *Journ. Geoph. Soc. Lon*, **vol 142**, (1985), 711 pp.

Jones, W.B., and Lippard, S.J.,: New age determination and geology of Kenya rift-Nyanzian rift junction, west Kenya. *Journ. of Geol. Soc.Lon* **vol 136** (1979) pg 63.

Kanda, I.,: Geochemical exploration of geothermal prospects: A case study of Menengai, Kenya , Presented at Short Course VI on Exploration for Geothermal Resources, organized by *UNU-GTP, GDC and KenGen*, at Lake Bogoria and Lake Naivasha, Kenya (2011)

Lagat, J., Mbua, P., Mutria, C.,: Menengai prospect: Investigations for its geothermal potential." *GDC internal report* (2010), 64pp

Leat, P.T.,: The structural and Geochemical Evolution of Menengai caldera volcano, Kenya Rift Valley. *PhD Thesis, University of Lancaster, U.K.* (1983)

Leat, P.T.,: Geological evolution of the trachytic volcano Menengai, Kenya Rift Valley. *J Geol Soc London*, **141**: (1984), 1057-1069.

Leat, P.T.,: Discussion on the geological evolution of the trachytic caldera volcano Menengai, Kenya Rift Valley. *Journal of the Geological Society*, August 1, 1985; **142**(4): (1985), 711 - 712.

Leat, P.T., Macdonald, R, Smith, R.L,: Geochemical evolution of Menengai, Kenya Rift Valley. *J Geophys Res*, **89**: (1984), 8571-8592.

Lee, H.F., Yang, T.Y Lan, T. F. Chen, C.H, Song, S.R., Tsao, S.: Temporal variations of gas compositions of fumaroles in the Tatun Volcano Group, northern Taiwan, *Journal of Volcanology and Geothermal Research* **178**, (2008), 624-635

Macdonald, R., Navarro, J.M., Upton, B.G. J., Davies, G.R.,: Strong compositional zonation in peralkaline magma: Menengai, Kenya Rift Valley. *J. Volc Geotherm Res*, **60**: (1994), 301-325.

Marini, L.: Geochemical techniques for the exploration and exploitation of geothermal energy, *Viareggio Italy*. (2004)

Marini, L.: Interpretation of the geochemical data available for the Silali geothermal system (Kenya), *GDC unpublished internal report*, (2014)

Marini, L., and Fiebig, J.,: Fluid geochemistry of the magmatic-hydrothermal system of Nisyros (Greece), Review report of the Nisyros Island thermal fluids. (2004)

Martini, M.,: The forecasting significance of chemical indicator in areas of quiescent volcanism: examples from Vulcano and Phleorean Fields (Italy). In: Latter, J.H. (Ed.), volcanic Hazard. Springer, Berlin, pp. (1989), 372-383.

Mizutani, Y. and Matsuo, S. Successive observations of chemical components in the condensed water from a fumarole of Volcano Showa-shinzan. *Bull. Volcanol. Soc. Japan* **3**, (1959), 119–127 (in Japanese with English abstract).

Mungania, J., and Lagat, J., (editors), Mariita, N.O., Wambugu, J.M., Ofwona, C.O., Kubo, B.M., Kilele, D.K., Mudachi, V.S., Wanjie, C.K., Korio, R.K: Menengai volcano: Investigations for its geothermal potential." *KenGen Internal Report*, **93**, (2004),

Nehring, N.L., D'Amore, F., Gas chemistry and thermometry of the Cerro Prieto, Mexico, geothermal field. *Geothermics* **13**, (1984), 75–89.

Nicholson, K.,: Geothermal fluids: Chemistry and exploration techniques, Springer-Verlag Berlin Heidelberg New York ISBN 3-540-56017-3, (1993), pp.

Saito, G., Shinohara, H., and Kazahaya, K.,: Successive sampling of fumarolic gases at Satsuma-Iwojima and Kuju volcanoes, southwest Japan: Evaluation of short-term variations and precision of the gas sampling and analytical techniques, *Geochemical Journal*, **Vol. 36**, (2002) pp. 1 -20

Sekento, L.R.,: Geochemical and isotopic study of the Menengai geothermal field, Kenya. *UNU-GTP Publications, Report 31*, (2012), 769-792.

Shinohara, H., Giggenbach, W. F., Kazahaya, K. and Hedenquist, J. W. Geochemistry of volcanic gases and hot springs of Satsuma-Iwojima, Japan: Following Matsuo. *Geochem. J.* **27**, (1993), 271–285.

Shinohara, H., Composition of volcanic gases emitted during repeating Vulcanian eruption stage of Shimodake, Kirishima volcano, Japan, *Earth Planets Space*, **65**, (2013), 667–675

Taran, Yu.A., Hedenquist, J.F., Korzhinskii, M.A.,: Geochemistry of Magmatic Gases From Kudryavy Volcano, Iturup, Kuril Islands, *Geochim. Cosmochim. Acta*, **59**, (1995), pp. 1749–1761

Tassi, F.,Vaselli, O., Capaccioni, B., Macias, J. L., Nencetti, A., Montegrossi, G.,.. Magro, G.,: Chemical composition of fumarolic gases and spring discharges from El Chichón volcano, Mexico: causes and implications of the changes detected over the period 1998-2000, *Journal of Volcanology and Geothermal Research* **123**, (2003), 105-121

Tedesco, D., Sabroux, J.C.: The determination of deep temperatures by means of the CO-CO<sub>2</sub>-H<sub>2</sub>-H<sub>2</sub>O geothermometer: an example using fumaroles in the Campi Flegrei, Italy. *Bull. Volcanol.* **49**, (1987), 381-387. system,

Williams, L.A.J., Macdonald, R., Chapman, G.R., Late Quaternary caldera volcanoes of the Kenya Rift Valley. *J Geophys Res*, **89**: (1984), 8553-8570.